



Cite this: *Nanoscale*, 2020, **12**, 22928

Received 10th August 2020,  
Accepted 23rd October 2020

DOI: 10.1039/d0nr05879c

[rsc.li/nanoscale](https://rsc.li/nanoscale)

## An *in situ* and real time study of the formation of CdSe NCs†

Cristina Palencia,<sup>†</sup><sup>a,b</sup> Robert Seher,<sup>†</sup><sup>a,b</sup> Jan Krohn,<sup>a</sup> Felix Thiel,<sup>a,b</sup>  
 Felix Lehmkuhler<sup>b,c</sup> and Horst Weller<sup>a,b</sup>

**Magic Size Clusters (MSCs) have been identified in the last few years as intermediates in the synthesis of nanocrystals (NCs), and ever since there has been increased interest in understanding their exact role in the NC synthesis. Many studies have been focused on understanding the influence of precursors or ligands on the stability of MSCs and on whether the presence of MSCs influences the reaction pathway. However, their kinetic nature calls for an *in situ* temporal evolution study of the reaction, from the first seconds until the formation of regular nanocrystals, in order to unravel the role of MSCs in the formation of NCs. We have studied the synthesis of CdSe nanocrystals (NCs) in a continuous-flow reactor with *in situ* optical and small angle X-ray scattering characterization (SAXS). Our results show that MSCs are always formed, regardless the temperature, as necessary intermediates in the formation of CdSe NCs, and that their accumulation in solution depends only on the reaction time. These results explain why MSCs were, in some cases, not observed in some previous studies.**

The fast evolution of nanocrystal science has prompted scientists to use classical concepts from colloidal chemistry to describe nucleation and growth events in nanocrystals. However, in the last few years it has been shown that the classical nucleation theory and the LaMer model are not sufficient to explain the nucleation and growth of nanocrystals from their precursors in solution. One reason is that the classical nucleation theory basically considers the thermodynamic work to create a new surface, while nanocrystals are reaction-driven nucleation systems, since their formation entails not only the development of a solid from a liquid, but is the result of a

chemical reaction.<sup>1</sup> The formation kinetics of NCs comprise a rather complicated chemistry, in which several reaction intermediates can be formed and could follow different reaction pathways depending on reaction conditions.<sup>2–8</sup> In particular, Magic-Size Clusters (MSCs) have been identified to be intermediates in the formation of NCs. The term MSCs refers mainly to nanostructures below 2 nm that show extremely narrow absorption peaks, present quantized growth,<sup>9</sup> and occupy local minima in the free energy curve. These properties of MSCs as well as their role as building block units to form NCs cannot be explained by the classical nucleation theory.<sup>10</sup> Intense research work has been devoted to study MSCs. In many cases MSCs were observed at low temperatures, as a result of lowering the reaction kinetics.<sup>4,5,11,12</sup> Under different conditions, they have also been observed as intermediates to regular NCs at high temperatures.<sup>3,8</sup> In the same line, different authors have also reported on the influence of the precursor reactivity and ligands on the formation and stabilization of MSCs and have shown that quantized growth is highly impacted by synthetic conditions.<sup>3,8,13–17</sup> Consequently, in these and other studies, the authors have tried to investigate the role played by MSCs in the formation of NCs. For example, Kudera *et al.* have reported the sequential growth of MSCs,<sup>18</sup> and others suggested that MSCs act as monomer reservoirs or that they are, in fact, dead-ends in the formation of regular NCs.<sup>3,7,8,12,14</sup> Despite the efforts, the implication of MSCs in the synthesis of NCs is still not clear. This can be due to the many different precursors and ligands studied, which influence not only the kinetics, but also the thermodynamics of the reaction. To the best of our knowledge, a growth mechanism able to explain the experimental evidence gathered under very different experimental conditions and to group them has not been established yet.

We consider that there are two main difficulties to tackle in studying the nucleation and growth of nanocrystals. First of all, formation events are very fast processes that can occur in the millisecond to second time scale. Secondly, nanocrystals' properties and stability are mainly dictated by their surface,

<sup>a</sup>Department of Physical Chemistry, University of Hamburg, Grindelallee 117, 20146 Hamburg, Germany. E-mail: [cristina.palencia.ramirez@chemie.uni-hamburg.de](mailto:cristina.palencia.ramirez@chemie.uni-hamburg.de)

<sup>b</sup>The Hamburg Centre for Ultrafast Imaging, Luruper Chaussee 149, 22761 Hamburg, Germany

<sup>c</sup>Deutsches Elektronen-Synchrotron (DESY), Notkestrasse 85, 22607 Hamburg, Germany

†Electronic supplementary information (ESI) available: Experimental details. See DOI: 10.1039/d0nr05879c

‡These authors contributed equally to this article.



and therefore any disruption in the initial colloidal stability of the system (including the ones performed in the conventional purification steps prior to characterization) could alter the results. For these reasons, we believe that in order to obtain reliable information it is needed to access and control, with high precision, very small time windows along the reaction, without performing any change in the reaction mixture. Based on this, we have performed our experiments in a continuous-flow reactor, which enables both the synthesis and *in situ* characterization of MSCs and NCs with precise control of the reaction time. Characterization is performed *in situ* on the reaction media, with no further purification processes. This continuous-flow reactor is not only optimal to perform *in situ* characterization on an evolving reaction, but also has high reproducibility and mass-production capability. Indeed, other authors have hypothesized before the benefits of such devices.<sup>19–21</sup> The reactor transforms the classical hot-injection approach into a continuous process by separating nucleation and growth spatially between a very low volume nucleation chamber and a larger volume growth oven. *In situ* optical absorption and synchrotron X-ray based characterization is achieved upon coupling the reactor to an optic flow cell connected to a UV-VIS spectrometer and to a Kapton-based X-ray flow cell. A schematic of the reactor, as well as the main components, can be found in the ESI.†

In this work we aim at studying the implication of MSCs in the growth of regular NCs. Several studies have shown the

influence of the nature of precursors and ligands on the stability of MSCs. We present a preliminary study of MSC growth kinetics, based on *in situ* and real time studies performed in a continuous-flow reactor. To this aim, we have monitored the temporal evolution of the reaction from the mixture of the precursors till the formation of regular NCs by performing *in situ* characterization at very precise reaction times without disrupting the colloidal media, which ensures no alteration of the results due to purification steps. Our experiments are based on the variations of nucleation and growth temperature and reaction time. In our opinion, these preliminary and new studies will shed light on the role played by MSCs in the formation of regular NCs.

In all the experiments performed the precursors' composition and ratio as well as the ligands and solvent were kept constant. TEM characterization was performed *ex situ* on the obtained regular CdSe NCs confirming that they present a crystalline, spherical shape. The average diameter was 3.6 nm (350 °C, 7.6 s), in accordance with the first absorption maximum (572 nm).<sup>29</sup> The experimental details as well as the TEM images of the CdSe NCs can be found in the ESI.†

Fig. 1 shows a collection of absorption spectra measured *in situ*, at a growth time of 14 s, during the syntheses of CdSe NCs from their precursors. Each graph contains the spectra of experiments performed at the same nucleation temperature and different growth temperatures (equal to or lower than the



Fig. 1 *In situ* UV-VIS absorption spectra during the syntheses of CdSe NCs. Each graph contains ten spectra:  $t_{\text{nuc}} = t_{\text{growth}}$ , in brown. The spectra in the following colours (to the blue) belong to decreasing growth temperatures, in steps of 10 °C. The growth time in each case is 14 s. Dashed rectangles indicate the presence of MSCs-437.



nucleation temperature). In addition to the excitonic absorption peak characterizing continuously growing NCs, fixed absorption maxima located at 437 nm are observed in the nucleation temperature window between 270 °C and 300 °C (marked with dashed rectangles in Fig. 1). These maxima do not shift to higher wavelengths at higher growth temperatures, as expected for regular NCs. Instead, they show increasing intensity with higher growth temperatures. The relatively small full width at half maximum (FWHM) and the static position of the peaks evidence that they correspond to MSCs, in particular to the cluster family CdSe-437. The term MSC family is used to refer to the single species of MSCs. Since in many cases the exact composition and structure of MSCs remain unclear, the formula and characteristic absorption maximum are used to refer to a MSC family (*i.e.* CdSe-437 refers to CdSe MSCs with an absorption maximum at 437 nm). The stepwise formation of distinct species correlates with the typical behavior of MSCs. At the reaction times under study, 14 s, CdSe-437 is not observed at temperatures over 300 °C or below 270 °C, but only in the temperature window of 270 °C  $\leq T \leq$  300 °C. The observation that MSCs are formed in the syntheses of CdSe NCs only at intermediate, mild temperatures is intriguing. Aiming at elucidating the reason for that, we explored shorter reaction times and found that, in fact, MSCs are also formed at lower and higher temperatures. We observed their accumulation in the reaction mixture by monitoring the reaction at 4.5 s reaction time: Fig. S2† shows *in situ* absorption spectra at 260 °C, 280 °C and 350 °C. It is worth noting that at the intermediate temperatures both MSCs and regular NCs are observed at shorter (4.5 s) and longer (14 s) reaction times. This will be discussed later. Although CdSe-437 is the most persistent MSC observed, other MSC families were also found when monitoring the reaction at 4.5 s. This is indeed in agreement with previous reports, which show that room temperature syntheses lead to the formation of one single MSC family, whereas different MSC families are obtained if the reaction temperature is higher than 120 °C.<sup>17</sup>

To further corroborate the formation of MSCs we have performed *in situ* small angle X-ray scattering (SAXS) measurements at the beamline ID02 at ESRF (Grenoble, France).<sup>22</sup> In these experiments the nucleation temperature was varied between 190 °C and 280 °C and the growth temperature was kept constant at 230 °C. In order to explore even smaller reaction times, the analysis was performed at a reaction time of 1.5 s. The relative volume fractions of CdSe species observed in the Monte Carlo fits obtained from the SAXS data (Fig. 2) evidence the quantized growth in steps characteristic of the presence of MSCs.<sup>23</sup> A growth step of MSCs is evident from the change in radius from  $r = 0.87$  nm to  $r = 0.94$  nm upon increasing the nucleation temperature from 190 °C to 200 °C. Subsequently, the mean radius does not change until a temperature of 230 °C, at which a shoulder corresponding to an NC radius of 1.02 nm is formed. This shoulder is fully pronounced at 240 °C. A further temperature increase to 250 °C and above causes the onset of continuous growth of the NCs. This is also in agreement with the *in situ* optical experiments shown in

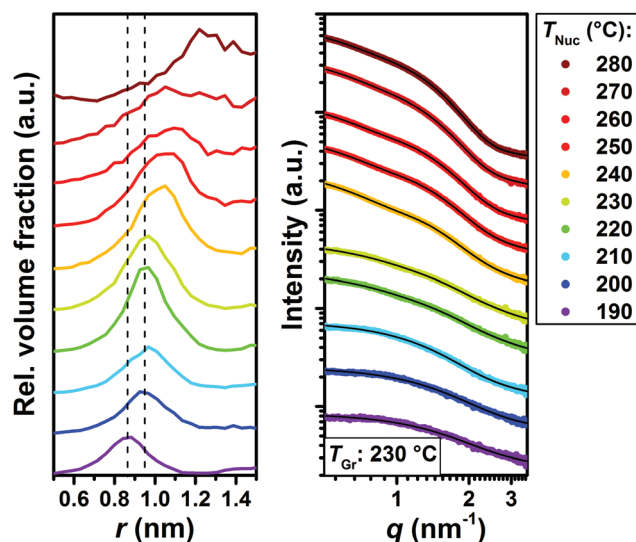


Fig. 2 Left: Relative volume fractions of different CdSe species obtained from Monte Carlo fitting of the SAXS patterns shown in the left side. Quantized growth from  $r = 0.87$  nm until  $r = 0.94$  nm and 1.02 nm, followed by continuous growth with nucleation temperatures higher than 240 °C. The curves are vertically offset for clarity. Right: SAXS patterns obtained at a reaction time of 1.5 s and a growth temperature of 230 °C, with varying nucleation temperature.

Fig. S2,† in which the onset of continuous growth can be linked to the broadness of the absorption curves.

Likewise, SAXS can provide information regarding the mesophase formation during the nucleation and growth of NCs, since mesophases display clear Bragg peaks in the SAXS regime. It is worth noting that in the last few years the formation of mesophases has been reported to stabilize MSCs and, since our results show that MSCs can be found in solution regardless the reaction temperature, it is important to investigate if the reaction mixture can form mesophases prior to nucleation. As blank experiments (Fig. 3), we investigated the SAXS patterns of the precursor mixture (prior nucleation) at room temperature, 50 °C and 100 °C. Two distinct Bragg peaks at 1.84 nm<sup>-1</sup> and 3.69 nm<sup>-1</sup> characterize the SAXS patterns at room temperature, whose intensity decreases at 50 °C until they vanish at 100 °C. It is worth noting that the second Bragg peak is found at the double  $q$  value of the first, indicating the same periodicity (the second peak is therefore assigned to the second order reflection). We attribute such Bragg peaks to the formation of a periodic structure in the precursor mixture, which is in consonance with previous literature.<sup>24</sup> Additional SAXS patterns recorded for each of the precursors individually show that in fact such a mesophase is formed in the Cd precursor. The increased scattering intensity of the Cd precursor below 1 nm<sup>-1</sup> with a broad maximum at around 0.2 nm<sup>-1</sup> to 0.3 nm<sup>-1</sup> indicates the presence of an additional structure. This is in good agreement with the findings by Abécassis *et al.*,<sup>24</sup> who reported the formation of a lamellar mesophase in the Cd-myristate solution at room temperature, which melts upon heating to 100 °C, and by the Buhro



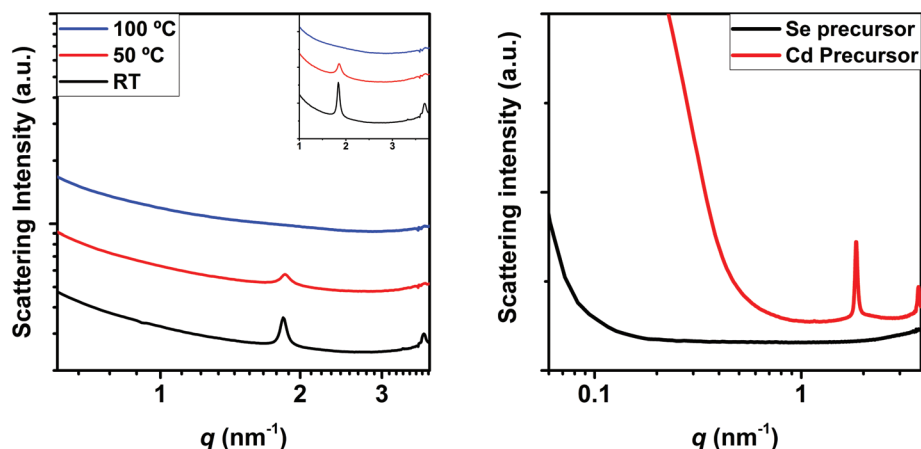


Fig. 3 Left: SAXS patterns of the precursor mixture at different temperatures prior to nucleation. The inset shows a magnification of the Bragg peaks observed above  $1 \text{ nm}^{-1}$ . Right: Scattering curves of the individual Cd and Se precursors.

group,<sup>25–27</sup> who showed the formation of a lamellar mesophase composed of the precursor, prior to the formation of MSCs. As reported recently by Nevers *et al.* and Cunningham *et al.*, mesophase formation would contribute to the stabilization of MSCs.<sup>6,28</sup> As found by Zhang *et al.*<sup>12</sup> these pre-nucleation structures would not present any covalent bonds, and only dispersive interactions would link the precursors. This would be borne out by the fact that such structures melt at intermediate temperatures. The facts that the precursor mixture shows mesophase formation at low temperatures and that such a mesophase melts at temperatures below the nucleation temperature indicate that MSCs formation might be temperature independent, as supported by our optical and SAXS results.

These experiments clearly evidence that MSCs are always intermediates in the syntheses of CdSe NCs, and that whether they are accumulated in solution or not depends on the reaction time. Utilizing size-selective precipitation of a reaction mixture obtained at  $350^\circ\text{C}$  and 4.5 s reaction time we could separate and isolate five different fractions, containing distinct

CdSe species. Assuming a spherical particle shape, an aggregation number  $N_{\text{CdSe}}$  was determined for each species using a particle diameter ( $d_{\text{Abs}}$ ) determined from the sizing curve published by Yu *et al.*<sup>29</sup> The corresponding absorption spectra are depicted in Fig. 4, which also contains a table resuming the particle diameters and calculated aggregation numbers. The MSC diameters determined from the sizing curve and from the SAXS patterns fit reasonably well. The MSCs observed by SAXS (diameters 1.74 nm, 1.88 nm and 2.04 nm) match the three largest MSCs observed in the optical spectra: 403 nm, 437 nm and 465 nm (diameters 1.58 nm, 1.85 nm and 2.06 nm). Smaller sizes below  $\sim 1.6$  nm could not be accessed from the SAXS results because of the limitations of resolution and scattering strength of the small particles. Small deviations between SAXS and UV-VIS have also been found by other authors.<sup>24</sup> These selective precipitation experiments evidence that the reaction mixtures obtained *in situ* contain different MSC families.

Our results show that MSCs are always formed as necessary intermediates during the synthesis of CdSe NCs, regardless



$\lambda$ (nm)	$d_{\text{Abs}}$ (nm)	$N_{\text{CdSe}}$	MSC species
350	1.09	12	(CdSe) <sub>13</sub>
380	1.37	25	(CdSe) <sub>19</sub>
403	1.58	38	(CdSe) <sub>33</sub>
437	1.85	61	(CdSe) <sub>66</sub>
467	2.06	84	—

Fig. 4 Absorption spectra for the fraction obtained by size selective precipitation from the reaction mixture at  $350^\circ\text{C}$  and 4.5 s. The table shows the absorption maxima of the CdSe species, their diameters and the calculated aggregation numbers. *Fi* is the initial sample and F1, ..., F5 the consecutive fractions obtained.





the temperature. We have also observed that their accumulation in solution depends on the reaction time. These results indicate a monomer-driven growth mechanism that governs both the quantized growth (from smaller to larger MSCs) and the continuous growth, characteristic of regular NCs. We propose that the monomer source is temperature dependent, as explained hereafter. The formation rate of MSCs ( $r_{\text{MSC}}$ ) is directly proportional to the concentration of nuclei ( $[\text{Nucl.}]$ ) and the concentration of free monomers in solution ( $[\text{M}]$ ) and can be written, in general, as

$$r(\text{MSCs}) = k \times [\text{Nucl.}] \times [\text{M}]$$

At mild temperatures ( $T \leq 260^\circ\text{C}$ ) the nucleation rate is low and subsequently, the concentration of MSCs formed as well. The small nucleation rate leaves a high concentration of monomers  $[\text{M}]$  in solution. During the very first seconds ( $t \leq 4.5$  s), these monomers are attached to the smallest MSCs, forming other cluster families:

$$r(403) = k(403) \times [\text{Nucl.}] \times [\text{M}];$$

$$r(437) = k(437) \times [403] \times [\text{M}];$$

$$r(465) = k(465) \times [437] \times [\text{M}];$$

$$r(\text{NCs}) = k(\text{NCs}) \times [465] \times [\text{M}]$$

As has been mentioned before, in all of our experiments CdSe-437 is the most persistent MSC, indicating either its higher stability in comparison with other MSC families or its fastest formation ( $k(437) > k(465)$ ). As seen in Fig. 1, at longer reaction times (14 s) at these mild temperatures ( $T \leq 260^\circ\text{C}$ ) regular NCs are observed in solution rather than MSCs. We rationalize this in terms of a monomer-driven continuous growth that forms NCs from MSCs by monomer addition. The monomer source comes from the unreacted monomers after nucleation. In this way, MSCs are accumulated in solution only in the first seconds after their nucleation, and the additional monomers in solution grow into larger MSCs (during the very first seconds, see Fig. S2†) and into regular NCs at longer reaction times (Fig. 1). Temperatures above  $300^\circ\text{C}$  induce a high nucleation rate, and consequently the concentration of MSCs formed is high and the monomer concentration is low. The formation rates can be written analogously as follows:

$$r(382) = k(382) \times [\text{Nucl.}] \times [\text{M}];$$

$$r(437) = k(437) \times [382] \times [\text{M}];$$

$$r(465) = k(465) \times [437] \times [\text{M}];$$

$$r(\text{NCs}) = k(\text{NCs}) \times [465] \times [\text{M}]$$

or

$$r(\text{NCs}) = k(\text{NCs}) \times [\text{Nucl.}] \times [\text{M}]$$

The relatively low availability of monomers after nucleation seems to suffice to produce the monomer-driven quantized growth from smaller to larger MSCs. In consequence, MSCs can be observed in solution only in the very first seconds

(Fig. S2†). This monomer depletion, together with the high temperatures, is the driving force that causes the dissolution of MSCs.<sup>3,8,12,14</sup> At longer reaction times (14 s, Fig. 1) the absorption spectra show absorption peaks characteristic of regular NCs. Under these conditions a monomer driven growth from MSCs to NCs seems reasonable, while the systems enter a typical Ostwald ripening process. However, we cannot discard a secondary nucleation event following the dissolution of MSCs. This is the result observed in many regular hot injection syntheses of CdSe and other NCs, in which MSCs are not observed, because short reaction times are usually not investigated. Performing the synthesis in a continuous-flow reactor, which enables access to short time scales, has allowed these findings to be obtained.

The interplay of reaction parameters creates a small temperature window ( $260^\circ\text{C} < T \leq 300^\circ\text{C}$ ) in which the relative reaction rates result in a temporary accumulation of MSCs in solution. Under these circumstances, MSCs coexist with regular NCs both at shorter (4.5 s, Fig. S2†) and longer reaction times (14 s, Fig. 1). Under these conditions, the dissolution of MSCs does not take place, given that the temperatures might not be high enough and that there is no drastic monomer depletion.

The formation rates can be written as follows:

$$r(403) = k(403) \times [\text{Nucl.}] \times [\text{M}];$$

$$r(437) = k(437) \times [403] \times [\text{M}];$$

$$r(\text{NCs}) = k(\text{NCs}) \times [403] \times [\text{M}]$$

The monomer source for the growth of smaller MSCs into larger MSCs (CdSe-403 to CdSe-437) and into NCs comes from the monomers left after nucleation. At these temperatures, the monomer excess is consumed not only in the formation of CdSe-437, but also in the formation of regular NCs. Since CdSe-437 coexists with regular NCs, we propose that they grow from monomer addition from smaller, more unstable MSCs (CdSe-403). It is worth noting that in this temperature window, longer reaction times do not alter notably the reaction mixture composition (CdSe-437 coexists with NCs at both 4.5 s and 14 s). We suggest that this is due to the higher stability of CdSe-437 and the temperatures, which seem to not be high enough to cause MSC dissolution. Interestingly, the effect observed for the reaction time is the growth of NCs: from 490 nm at 4.5 s (Fig. S2†) to 527 nm at 14 s (Fig. 1, nucleation at  $280^\circ\text{C}$ , brown curve). This NC growth evidences that the monomer availability after nucleation is sufficient for the growth from MSCs into NCs. Despite the larger monomer availability at lower temperatures ( $T \leq 260^\circ\text{C}$ ), growth into NCs does not occur at smaller reaction times, presumably due to the low temperatures. To better support our proposed monomer-driven mechanism in which the monomer source is affected by the temperature, we have monitored the growth of MSCs at different temperatures ( $260^\circ\text{C}$ ,  $280^\circ\text{C}$  and  $350^\circ\text{C}$ ) at different reaction times (Fig. S3†). Increasing reaction times result in an overall increase of the optical density, which indicates the presence of



monomers in the reaction media, confirming our mechanism of a monomer-driven growth. The formation of MSCs is a dynamic equilibrium in which both kinetics and thermodynamics play a role. The existence of a certain MSC family (*i.e.* CdSe-437) is the result of the interplay between its stability and formation rate.

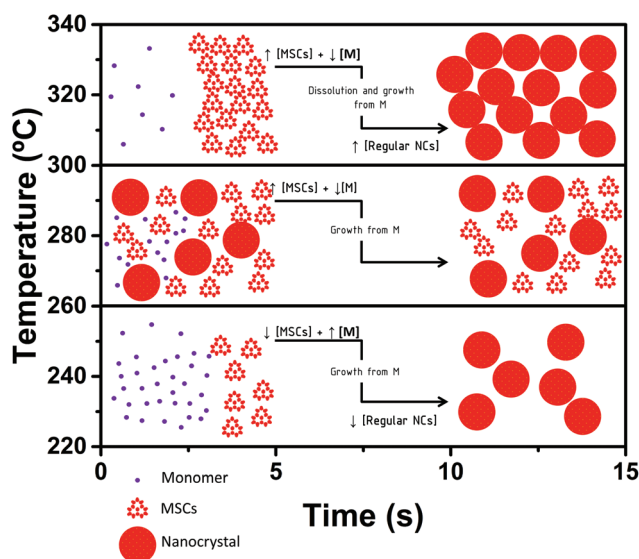
Scheme 1 shows the proposed growth mechanism. These results are in contrast to the results obtained by Zhang *et al.*,<sup>3,12</sup> who showed MSCs as dead-ends in the formation mechanism of regular NCs. According to their results, MSCs are intermediates of regular NCs, but the formation pathway includes the dissolution of MSCs to form either immediate precursors or fragments, able to lead to the formation of regular NCs. Our preliminary results show that dissolution may occur at high temperatures and is driven by monomer depletion. We propose that high temperatures, as the ones used in regular hot injection syntheses, and monomer depletion cause MSC dissolution. Our results unify the processes underwent by MSCs at low and high temperatures and clearly show that MSCs are intermediates in the formation of regular NCs regardless the synthesis temperature for the system studied. We have found that, for the studied system, MSCs can be observed at reaction times as short as 1.5 s, 4.5 s or 14 s. Based on this and previous studies, we suggest that the MSC formation and dissolution are in dynamic equilibrium, changing constantly during the evolution of the reaction, and that this equilibrium may be mainly influenced by the reaction temperature, which directly influences the monomer formation and depletion and could, therefore, force the monomer dissolution. Findings by other authors,<sup>3,8,14</sup> who have reported on the high stability of MSCs at high tempera-

tures in solution over time, are not contradictory to our findings, if this fast equilibrium between MSCs and monomers is considered. Our conclusions are also in line with the recent report by Cunningham *et al.*<sup>28</sup> in which the authors reported on the influence of the thermal energy on the reaction pathways of ZnSe NCs. Here we observe how the thermal energy affects the monomer concentration in solution and, subsequently, determines the reaction mixture composition. Our new formation model, based on the reaction temperature and time, supports that MSCs could dissolve releasing free monomers that will cause the growth into regular NCs, at high enough temperatures. Indeed, it also explains why MSC intermediates are not usually observed in hot-injection-type syntheses of CdSe NCs, but observed at low temperatures. In typical batch syntheses the first few seconds of the reaction cannot be investigated in a reproducible manner, since the sample taking is limited by the operator, and precision and reproducibility at these short times are problematic. In addition, the usual temperatures needed for hot injection syntheses accelerate the kinetics and cause MSC dissolution, masking the existence of MSCs in solution. Considering this, it is worth noting that performing the growth experiments in a continuous-flow reactor has been crucial to observe the accumulation of MSCs in solution at very small reaction times and to our proposed mechanism, and it provides tremendous possibilities to study nucleation and growth.

## Conclusions

In this communication we have presented a new approach to study the formation dynamics of NCs based on *in situ* characterization. This approach allows studying the reaction at very short and precise reaction times without altering the reaction medium. We have studied the formation of CdSe NCs from their precursors by monitoring the reaction at different temperatures and reaction times from 1.5 s to 14 s. We have shown that it is possible to observe and isolate MSCs at different temperatures, if the monitored reaction time is short enough. In the formation of CdSe NCs we have found a temperature window between 260 °C and 300 °C in which MSCs are accumulated in solution at shorter and longer reaction times. At lower and higher temperatures there is no presence of MSCs at such longer reaction times, since MSCs have grown into regular NCs. However, MSCs could be observed at lower reaction times. We have demonstrated that the accumulation of MSCs in solution depends on the reaction temperature and time and suggest that this is due to an interplay of thermodynamics and kinetics, mainly influenced by the reaction temperature.

Our results have strong implications in the classical nucleation theory: the unequivocal formation of MSCs introduces local minima in the free energy curve for nucleation and growth, deviating for the classical smooth free energy curve for the formation of regular NCs. This is the first time that MSCs are reported as intermediates under a wide range of reaction



**Scheme 1** Formation of MSCs and NCs at different reaction times and temperatures. Small blue circles represent monomers, orange tetrahedra represent MSCs, and red circles represent NCs. For clarity, the scale between monomers, MSCs and NCs has not been considered. The schemes are depicted at the monitored reaction times of 4.5 and 14 s.



conditions for the same system and evidence that MSCs are formed independent of the reaction temperature as intermediates to regular NCs. The results presented here are part of our current investigations focused on investigating the nucleation and growth of nanocrystals.

These successful experiments have been only possible by performing the synthesis and *in situ* characterization in our proprietary continuous-flow reactor.<sup>30</sup> This is strong evidence of the need for *in situ* studies to unravel the formation dynamics of nanocrystals. We consider that the innovative approach presented here is exceptionally advantageous to perform investigations on nucleation and growth in NCs.

## Conflicts of interest

There are no conflicts to declare.

## Acknowledgements

The authors acknowledge the support in the beamtime experiments to Dr. Sebastian Bommel, Dr. Mohammad Vakili, Dr. Lara Frenzel and Prof. Martin Trebbin. This work has been supported by the excellence cluster “The Hamburg Centre for Ultrafast Imaging – CUI” of the Deutsche Forschungsgemeinschaft (DFG) – EXC 1074 – project ID 194651731 and the Cluster of Excellence “CUI: Advanced Imaging of Matter” of the Deutsche Forschungsgemeinschaft (DFG) – EXC 2056 – project ID 390715994. Cristina Palencia also thanks the Christiane Nüsslein-Volhardt and the L'Oréal for Woman in Science Foundation for their support. In addition, we also acknowledge the European Synchrotron Radiation Facility (ESRF) for provision of synchrotron radiation facilities and Johannes Möller for assistance at beamline ID02, as well as Jacques Gorini for technical support.

## Notes and references

- M. A. Wall, B. M. Cossart and J. T. C. Liu, *J. Phys. Chem. C*, 2018, **122**, 9671.
- K. Yu, M. Z. Hu, R. B. Waing, M. Le Piolet, M. Frotey, M. B. Zaman, X. H. Wu, D. M. Leek, Y. Tao, D. Wilkinson and C. S. Li, *J. Phys. Chem. C*, 2010, **114**, 3329.
- Z. J. Jiang and D. F. Kelley, *ACS Nano*, 2010, **4**, 1561.
- B. M. Cossart and J. S. Owen, *Chem. Mater.*, 2011, **23**, 3114.
- S. Dolai, P. Dutta, B. B. Muhoberac, C. D. Irving and R. Sardar, *Chem. Mater.*, 2015, **27**, 1057–1070.
- D. R. Nevers, C. B. Williamson, B. H. Savitzky, I. Hadar, U. Banin, L. F. Kourkoutis, T. Hanrath and R. D. Robinson, *J. Am. Chem. Soc.*, 2018, **140**, 3652.
- Y. Y. Liu, M. Willis, N. Rowell, W. Z. Luo, H. S. Fan, S. Han and K. Yu, *J. Phys. Chem. Lett.*, 2018, **9**, 6356.
- N. Kirkwood and K. Boldt, *Nanoscale*, 2018, **10**, 18238.
- S. M. Harrell, J. R. McBride and S. J. Rosenthal, *Chem. Mater.*, 2013, **25**, 1199.
- J. Lee, J. Y. Yang, S. G. Kwon and T. Hyeon, *Nat. Rev. Mater.*, 2016, **1**, 16034.
- Z. A. Peng and X. Peng, *J. Am. Chem. Soc.*, 2002, **124**, 3343.
- B. Zhang, T. Zhu, M. Ou, N. Rowell, H. Fan, J. Han, L. Tan, M. T. Dove, Y. Ren, X. Zuo, S. Han, J. Zeng and K. Yu, *Nat. Commun.*, 2018, **9**, 2499.
- K. Yu, M. Z. Hu, R. Wang, M. Le Piolet, M. Frotey, Md. B. Zaman, X. Wu, D. M. Leek, Y. Tao, D. Wilkinson and C. Li, *J. Phys. Chem. C*, 2010, **114**, 3329.
- D. C. Gary, M. W. Terban, S. J. L. Billinge and B. M. Cossart, *Chem. Mater.*, 2015, **27**, 1432.
- E. Groeneveld, S. van Berkum, A. Meijerink and C. de Mello Donegá, *Small*, 2011, **7**, 1247.
- M. Li, J. Ouyang, C. I. Ratcliffe, L. Pietri, X. Wu, D. M. Leek, I. Moudrakovski, Q. Lin, B. Yang and K. Yu, *ACS Nano*, 2009, **3**, 3832.
- C. M. Evans, A. M. Love and E. A. Weiss, *J. Am. Chem. Soc.*, 2012, **134**, 117298.
- S. Kudera, M. Zanella, C. Giannini, A. Rizzo, Y. Li, G. Gigli, R. Cingolani, G. Ciccarella, W. Spahl, W. J. Parak and L. Manna, *Adv. Mater.*, 2007, **19**, 548.
- X. G. Peng, J. Wickham and A. P. Alivisatos, *J. Am. Chem. Soc.*, 1998, **120**, 5343.
- S. Marre, J. Park, J. Rempel, J. Guan and M. G. Bawendi, *Adv. Mater.*, 2008, **20**, 4830.
- J. Baek, Y. Shen, I. Lignos, M. G. Bawendi and K. F. Jensen, *Angew. Chem., Int. Ed.*, 2018, **57**, 10915.
- T. Narayanan, M. Sztucki, P. Van Vaerenbergh, J. Leonardon, J. Gorini, L. Claustre, F. Sever, J. Morse and P. Boesecke, *J. Appl. Crystallogr.*, 2018, **51**, 1511.
- I. Bressler, B. R. Pauw and A. F. Thunemann, *J. Appl. Crystallogr.*, 2015, **48**, 962.
- B. Abécassis, C. Bouet, C. Garnero, D. Constantin, N. Lequeux, S. Ithurria, B. Dubertret, B. R. Pauw and D. Pontoni, *Nano Lett.*, 2015, **15**, 2620.
- Y. H. Liu, F. D. Wang, Y. Y. Wang, P. C. Gibbons and W. E. Buhro, *J. Am. Chem. Soc.*, 2011, **133**, 17005.
- Y. Y. Wang, Y. H. Liu, Y. Zhang, F. D. Wang, P. J. Kowalski, H. W. Rohrs, R. A. Loomis, M. L. Gross and W. E. Buhro, *Angew. Chem., Int. Ed.*, 2012, **51**, 6154.
- Y. Y. Wang, Y. Zhang, F. D. Wang, D. E. Giblin, J. Hoy, H. W. Rohrs, R. A. Loomis and W. E. Buhro, *Chem. Mater.*, 2014, **26**, 2233.
- P. D. Cunningham, I. Coropceanu, K. Mulloy, W. Cho and D. V. Talapin, *ACS Nano*, 2020, **14**, 3847.
- W. W. Yu, L. Qu, W. Guo and X. Peng, *Chem. Mater.*, 2003, **15**, 2854.
- H. Weller and J. Niehaus, *Patent US 9084797B2*, 2015.

